

1 **Multi-trait genomic prediction improves selection accuracy for enhancing seed mineral**
2 **concentrations in pea (*Pisum sativum L.*)**
3 Sikiru Adeniyi Atanda¹, Jenna Steffes¹, Yang Lan¹, Md Abdullah Al Bari¹, Jeonghwa Kim¹, Mario
4 Morales¹, Josephine Johnson¹, Rica Amor Saludares¹, Hannah Worrall², Lisa Piche¹, Andrew
5 Ross¹, Michael A Grusak³, Clarice J. Coyne⁴, Rebecca J. McGee^{5,6}, Jiajia Rao¹, and Nonoy
6 Bandillo^{1*},

7

8 ¹ Department of Plant Sciences, North Dakota State University, Fargo, ND 58108-6050, USA

9 ² NDSU North Central Research Extension Center, 5400 Highway 83 South Minot, ND 58701,
10 USA

11 ³ USDA-ARS Edward T. Schafer Agricultural Research Center, 1616 Albrecht Boulevard N,
12 Fargo, ND 58102-2765

13 ⁴ USDA-ARS Plant Germplasm Introduction and Testing, Washington State University,
14 Pullman, WA 99164, USA

15 ⁵ USDA-ARS Grain Legume Genetics and Physiology Research, Pullman, WA 99164, USA

16 ⁶ Department of Horticulture, Washington State University, Pullman, WA 99164, USA

17

18 * Corresponding author: nonoy.bandillo@ndsu.edu

19 **ORCID**

20 SA: 0000-0001-8758-2063

21 NB: 0000-0002-5941-9047

22 MAG: 0000-0002-7976-3419

23 CJC: 0000-0003-1374-4618

24

25

26

27

28

29

30

31 **Abstract**

32 The superiority of multi-trait genomic selection (MT-GS) over univariate genomic selection (UNI-
33 GS) can be improved by redesigning the phenotyping strategy. In this study, we used about 300
34 advanced breeding lines from North Dakota State University (NDSU) pulse breeding program and
35 about 200 USDA accessions evaluated for ten nutritional traits to assess the efficiency of sparse
36 testing in MT-GS. Our results showed that sparse phenotyping using MT-GS consistently
37 outperformed UNI-GS when compared to partially balanced phenotyping using MT-GS. This
38 strategy can be further extended to multi-environment multi-trait GS to improve prediction
39 performance and reduce the cost of phenotyping and time-consuming data collection process.
40 Given that MT-GS relies on borrowing information from genetically correlated traits and relatives,
41 consideration should be given to trait combinations in the training and prediction sets to improve
42 model parameters estimate and ultimately prediction performance. Our results point to heritability
43 and genetic correlation between traits as possible parameters to achieve this objective.

44

45 **Key words:** Genomic selection, heritability, multi-trait, genomic best linear unbiased estimate,
46 sparse testing, genetic correlation, cross-validation

47

48

49

50

51

52

53

54

55

56 1.0 Introduction

57 In recent times, there is an increased demand for genetic improvement of nutritional traits in crops
58 due to the growing demand for plant-based protein, mineral elements and vitamins. Pulse crops
59 are known to have high protein value and are rich in micronutrients with potential to alleviate
60 hidden hunger (Mudryj et al. 2014; Wadhawan et al. 2021; Bari et al. 2021). However,
61 phenotyping/screening for nutritional traits such as protein, manganese, selenium, copper, zinc,
62 iron, potassium, phosphorus, magnesium and calcium is expensive and time consuming, especially
63 in the early yield testing stage with hundreds of lines to evaluate. This is a major limitation in a
64 public breeding program aiming to have a biofortified product profile. However, due to
65 advancement in the genotyping platform, the cost of genotyping is becoming relatively less
66 expensive compared to the cost of phenotyping; thus, genomic selection (GS) that uses whole-
67 genome information to predict genomic estimated breeding value (GEBV) of unobserved
68 genotypes is gaining traction as breeders' choice of selection method (Poland et al. 2012; Zhao et
69 al. 2021; Bassi et al. 2016; Santantonio et al. 2020; Atanda, et al. 2021a). Though GS research in
70 pea is scanty, the available studies (Annicchiarico et al. 2019; Crosta et al. 2021; Bari et al. 2021)
71 show GS potential to predict the genetic merit of pea lines and germplasm accessions. Following
72 Bari et al. (2021), the North Dakota State University (NDSU) pulse breeding program is
73 prioritizing the use of GS particularly in the preliminary yield trial (PYT or stage 1) where
74 effectiveness of phenotypic selection is limited by phenotyping in one/two locations due to seed
75 multiplication challenges for hundreds of lines for multi-location trials. Consequently, the NDSU
76 pulse breeding program is focused on redesigning the PYT from phenotypic based selection to GS
77 to reduce the number of seeds for phenotyping and increase selection accuracy for advancement
78 of promising lines to advanced yield testing stage.

79

80 In general, GS is often performed with univariate-trait (UT) models that assume genetic correlation
81 among traits to be zero (Jia and Jannink 2012; Montesinos-López et al. 2016, 2018; Bhatta et al.
82 2020; Gaire et al. 2022). However, in practice, breeders' select for multiple traits that are
83 genetically correlated, ranging from negative to positive correlations. To harness the genetic
84 correlation between traits and among genotypes to improve prediction accuracy, multi-trait (MT)
85 models, which are the generalization of UT models, have been investigated. Several empirical
86 studies (Calus and Veerkamp 2011; Montesinos-López et al. 2018; Bhatta et al. 2020; Gaire et al.
87 2022) have reported improved prediction accuracy in different crops using MT models that allow
88 borrowing of information between correlated traits and among genotypes compared to UT models.
89 Prediction accuracy in MT-GS improves as correlation between traits increases (Jia and Jannink
90 2012; Okeke et al. 2017; Montesinos-López et al. 2018, 2019; Neyhart et al. 2019), however, trait
91 heritability varies and is a key limiting factor to upper bound of prediction accuracy (Manolio et
92 al. 2009; Yang et al. 2015; Schopp et al. 2017; Zhang et al. 2019; Atanda et al. 2021a). These
93 factors will likely influence the composition of traits in the training and the prediction sets in MT-
94 GS and ultimately the prediction accuracy.

95
96 In the MT-GS model, the training set consists of individuals with phenotypic records for all traits
97 to predict the genetic values of un-phenotyped individuals in the prediction set using genome-wide
98 marker information. The crucial question is how to design a MT-GS strategy that will optimize the
99 trade-off between the limiting factors and accuracy of predicting the genetic value of the traits.
100 Studies (Montesinos-López et al. 2016, 2018, 2019; Guo et al. 2014; Bhatta et al. 2020; Gaire et
101 al. 2022) have highlighted the importance of each factor to prediction accuracy; however, nothing
102 is known about their combinations on composition of traits in the training and prediction set in the
103 context of MT-GS. Consequently, we investigated the influence of the limiting factors on

104 composition of traits in the training and prediction sets to guide the use of MT-GS in a breeding
105 program.

106 Further, in most MT-GS cross-validation studies (Montesinos-López et al. 2016, 2018, 2019; Guo
107 et al. 2014; Bhatta et al. 2020; Gaire et al. 2022), the same set of genotypes overlap across traits
108 for testing prediction models (**Suppl. Fig. 1A, C**). In such a scenario, the same set of genotypes
109 have phenotypic records for all traits while the other genotypes serve as a prediction set (partially
110 balanced testing strategy, denoted as PBT); however, results from multi-environment GS studies
111 have shown that this approach is less optimal compared to sparse testing using genomic prediction
112 where phenotyping of genotypes is split across environments (Burgueño et al. 2012; Jarquin et al.
113 2020; Atanda et al. 2021). We extend sparse phenotyping in the context of MT-GS in which the
114 phenotyping of lines is split across traits (**Suppl. Fig. 1B, D**). This strategy could improve
115 prediction accuracy in MT-GS by efficiently using information across traits and genotypes. More
116 so, it can be robust for building historical data for use in prediction models, since all genotypes
117 have phenotypic records for the different traits. To further evaluate the potential of GS in the
118 NDSU pulse breeding program and how it can be efficiently deployed to improve genetic gain, the
119 following were our objectives in this study: 1) determine the efficiency of MT compared to UT in
120 predicting nutritional traits in pea, 2) determine the optimal method to design training and testing
121 trait sets using heritability and genetic correlation between traits as metric, and 3) identify optimal
122 resource allocation for phenotyping nutritional traits in the early yield testing stage by comparing
123 the predictive ability of sparse and partial balanced testing.

124

125

126

127

128

129 **2.0 Materials and Methods**

130 **2.1 Genetic Materials and Field or Greenhouse Evaluation**

131 The genetic material consisted of 282 pea lines (DS1) from North Dakota State University (NDSU)
132 pulse breeding program and 192 USDA pea accessions (DS2) previously described in Bari et al.
133 (2021). The NDSU lines were planted in augmented row-column design with five repeated checks
134 in the 2020-2021 growing season at the North Dakota Agricultural Experiment Station, Minot,
135 North Dakota, United States (27°29'N, 109°56'W). Seeds were treated with fungicide and
136 insecticide prior to planting. At planting, 30 seeds were planted on 152 × 60 cm plot size with 30
137 cm spacing between plots. Plots were harvested at physiological maturity (90-120 days after
138 planting) and dried to 15% moisture content. For the USDA pea accessions, six plants of each
139 accession were grown in 5L black plastic pots filled with a synthetic soil mix composed of two
140 parts Metro-Mix 360 (Scotts-Sierra Horticultural Products Co., Marysville, Ohio) and one part
141 vermiculite (Strong-Lite Medium Vermiculite, Sun Gro Horticulture Co, Seneca Illinois). Plants
142 were grown in a controlled environment greenhouse with a temperature regime of 22 ± 3 °C/day
143 and 20 ± 3 °C/ night, with a relative humidity ranging from 45% to 65% throughout the day/night
144 cycle. Sunlight was supplemented with metal halide lamps, set to a 15 h day, 9 h night cycle (lights
145 on at 700 h). In order to maintain an adequate supply of all mineral nutrients, a complete fertilizer
146 mixture was provided to each pot on a daily basis. Pots were irrigated with an automated drip
147 irrigation system (one drip line to each pot); the system was regulated with a timer that delivered
148 nutrient solution twice a day (younger plants) or three times a day (older plants) in sufficient
149 quantity to saturate the soil mass at each irrigation. The nutrient solution contained the following
150 concentrations of mineral salts: 1.0 mM KNO₃, 0.4 mM Ca(NO₃)₂, 0.1 mM MgSO₄, 0.15 mM
151 KH₂PO₄ and 25 µM CaCl₂, 25 µM H₃BO₃, 2 µM MnSO₄, 2 µM ZnSO₄, 0.5 µM CuSO₄, 0.5 µM
152 H₂MoO₄, 0.1 µM NiSO₄, 1 µM Fe(III)-N, N'-ethylenebis[2-(2-hydroxyphenyl)-glycine] (Sprint
153 138; Becker-Underwood, Inc., Ames, Iowa, USA). We thus attempted to maintain all essential

154 minerals at sufficient, but non-toxic levels, in the soil. Seeds were harvested from each accession
155 at full plant maturity.

156

157 **2.2 Mineral Analysis**

158 Mineral elements for DS1 were measured following procedures described in (Ma et al., 2017; Lan
159 et al. 2019). Briefly, 200g non-dehulled pea seeds were ground to fine flour and then digested with
160 concentrated nitric acid (70% HNO_3) in a digestion system block at 90 °C for 60 minutes.
161 Afterward, 3 mL of hydrogen peroxide was added to further the digestion process for 15 minutes,
162 followed by the addition of 3 mL hydrochloric acid (70% HCl) and heated for additional 5 minutes.
163 After cooling to room temperature, the digested samples were filtered through DigiFILTER (SCP
164 Science) and diluted to 10mL with nanopure water. To validate the procedure and analytical
165 measurement, an apple leaf standard (SRM 1515; National Institute of Standards and Technology,
166 Gaithersburg, Maryland, USA) was analyzed simultaneously with the pea flour samples. Total
167 concentration of the mineral elements was measured using inductively coupled plasma atomic
168 emission spectrometry (IRIS Advantage ICP-AES; Thermo Elemental, Franklin, Massachusetts,
169 USA). Mineral values were determined with the ICP-AES using the following spectral emission
170 lines (in nm): Ca, 184.0; Mg, 285.2; K, 769.8; P, 177.4; Fe, 238.2; Zn, 213.8; Mn, 260.5; Cu,
171 324.7; Ni, 231.6; B, 208.9; Mo, 202.0.

172

173 For the DS2, dried seeds (with seed coats) from 6 plants of each accession were ground to a
174 uniform powder using a coffee grinder with stainless steel blades. Two sub-samples of each
175 accession were weighed (approximately 200 mg each), dry ashed, resuspended in ultra-pure nitric
176 acid and analyzed for Ca, Mg, K, P, Fe, Zn, Mn, Cu, Ni, B and Mo concentrations using inductively
177 coupled plasma atomic emission spectrometry (IRIS Advantage ICP-AES; Thermo Elemental,
178 Franklin, Massachusetts, USA). Dry ashing was performed in quartz tubes, with samples ashed for

179 6 h at 450 °C. After cooling, to ensure complete oxidation of all tissues, 2.5 ml of 30% H₂O₂ was
180 added to each tube and samples were reheated to 450 °C for 1 h. Apple leaf standards (SRM 1515;
181 National Institute of Standards and Technology, Gaithersburg, Maryland, USA) were ashed and
182 analyzed along with pea seed samples to verify the reliability of the procedures and analytical
183 measurements. Mineral values were determined with the ICP-AES using the same spectral
184 emission lines (in nm) noted for the DS1 population.

185

186 **2.3 Genotyping**

187 Details on DNA isolation and genotyping-by-sequencing (GBS) can be found in Bari et al. (2021).
188 DS1 and DS2 were genotyped using GBS and 28, 832SNP markers were generated for DS1 while
189 380,527 SNP markers were generated for DS2. After removing SNPs with more than 90% missing
190 values, heterozygosity greater than 20% and with a minor allele frequency less than 5%, 11, 858
191 and 30, 645 SNPs remained for DS1 and DS2 respectively and were used for the analysis. Missing
192 SNPs were imputed with Beagle 5.1 (Browning et al., 2018).

193

194 **2.4 Phenotypic Data Analysis**

195 Best linear unbiased estimates of the phenotypes for DS1 accounting for spatial trend on the field
196 modelled by a smooth bivariate function of the spatial coordinates $f(\mathbf{r}, \mathbf{c})$ represented by 2D P-
197 splines was implemented in SpATS R package (Rodríguez-Álvarez et al. 2016). This was modeled
198 as:

199

200

201
$$\mathbf{y} = f(\mathbf{r}, \mathbf{c}) + \mathbf{X}\mathbf{b} + \mathbf{Z}_r\mathbf{u}_r + \mathbf{Z}_c\mathbf{u}_c + \boldsymbol{\varepsilon} \quad (1)$$

202

203 where: \mathbf{y} is the response variable for n-th phenotype, \mathbf{b} is the fixed effect of the genotype, \mathbf{u}_r and
204 \mathbf{u}_c are row and column random effects accounting for discontinuous field variation with
205 multivariate normal distribution: $\mathbf{u}_r \sim N(0, \mathbf{I}\sigma_r^2)$ and $\mathbf{u}_c \sim N(0, \mathbf{I}\sigma_c^2)$ respectively. \mathbf{I} is an identity
206 matrix and σ_r^2 and σ_c^2 are variance for row and column effect. $f(\mathbf{r}, \mathbf{c})$ is a smooth bivariate function
207 defined over the row and column positions (see Velazco et al. 2017 for details), $\boldsymbol{\epsilon}$ is the
208 measurement error from each plot with distribution of $\boldsymbol{\epsilon} \sim N(0, \mathbf{I}\sigma_\epsilon^2)$. \mathbf{I} is the same as above, σ_ϵ^2 is
209 variance for the residual term or simply referred to as nugget. \mathbf{X} and \mathbf{Z} are incidence matrix for the
210 fixed and random terms.

211

212 For the DS2, the mineral elements value of each accession was estimated as follows; mineral
213 values from the two sub-samples (see Mineral Analysis section for details) were averaged for each
214 accession; these averaged values are presented as ppm (parts per million), which is equivalent to
215 ug/g DW (micrograms per gram dry weight). In this study it was denoted as mean phenotypic
216 value of each accession for each mineral element. In general, the standard deviations for each
217 mineral were low (i.e., within each accession). Across all accessions, the average standard
218 deviation for each mineral (calculated as percent of the mean of the two sub-samples) was: Ca,
219 10.4%; Mg, 2.0%; K, 2.5%; P, 2.5%; Fe, 6.0%; Zn, 5.1%; Mn, 6.9%; Cu, 7.5%; Ni, 15.4%; B,
220 5.8%; Mo, 3.7%.

221

222

223

224

225

226

227

228 **2.5 Genomic Selection Models**

229 Univariate GS model was implemented in ‘BGLR’ R package (Pérez and de los Campos 2014)
230 using Bayesian ridge regression model equivalent to the genomic best linear unbiased prediction
231 (GBLUP) model expressed as:

232
$$\mathbf{y} = \mathbf{1}_k \mu + \mathbf{Z} \mathbf{u} + \boldsymbol{\varepsilon} \quad (2)$$

233
234 where \mathbf{y} is the vector ($n \times 1$) of adjusted means (BLUEs) using DS1 or mean phenotypic value
235 using DS2 for k -th genotypes for a given n -th trait/mineral element, μ is the overall mean and $\mathbf{1}_k$
236 ($k \times 1$) is a of vector ones, \mathbf{u} is the genomic effect of k -th genotypes assumed to follow multivariate
237 normal distribution expressed as $\mathbf{u} \sim N(0, \mathbf{G} \sigma_g^2)$. \mathbf{G} is the genomic relationship matrix and σ_g^2 is
238 the additive genetic variance.

239 MT-GS model was fit using Bayesian multivariate gaussian model in ‘MTM’ R package (de los
240 Campos and Grüneberg 2016). This is expressed as:

241
$$\begin{bmatrix} \mathbf{y}_1 \\ \vdots \\ \mathbf{y}_n \end{bmatrix} = \begin{bmatrix} \mathbf{1}_1 \mu_1 \\ \vdots \\ \mathbf{1}_k \mu_n \end{bmatrix} + \begin{bmatrix} \mathbf{Z}_1 & \cdots & 0 \\ \vdots & \ddots & \vdots \\ 0 & \cdots & \mathbf{Z}_n \end{bmatrix} \begin{bmatrix} \mathbf{u}_1 \\ \vdots \\ \mathbf{u}_n \end{bmatrix} + \begin{bmatrix} \boldsymbol{\varepsilon}_1 \\ \vdots \\ \boldsymbol{\varepsilon}_n \end{bmatrix} \quad (3)$$

242 where $\mathbf{y}_1 \dots \mathbf{y}_n$ are the vector of phenotypes, $\mu_1 \dots \mu_n$ are the overall mean for each n -th trait, \mathbf{Z}_1
243 $\dots \mathbf{Z}_n$ is the incidence matrix for genomic effect of the lines for each n -th trait, $\mathbf{u}_1 \dots \mathbf{u}_n$ is genomic
244 effect of the lines for each n -th trait and $\boldsymbol{\varepsilon}_1 \dots \boldsymbol{\varepsilon}_n$ is the residual error for each n -th trait. The random
245 term is assumed to follow multivariate normal distribution $[\mathbf{u}_1 \dots \mathbf{u}_n] \sim N[0, (\mathbf{G} \otimes \mathbf{G}_0)]$. Where
246 \mathbf{G} is the same as above and \mathbf{G}_0 is an unstructured variance-covariance matrix of the genetic effect
247 of the traits, this is represented as follows:

248

$$\mathbf{G}_0 \otimes \mathbf{G} = \begin{bmatrix} \sigma_{g_1}^2 & \sigma_{g_{12}} & \cdots & \sigma_{g_{1n}} \\ \sigma_{g_{21}} & \sigma_{g_2}^2 & \cdots & \cdots \\ \vdots & \ddots & \ddots & \vdots \\ \sigma_{g_{n1}} & \vdots & \cdots & \sigma_{g_n}^2 \end{bmatrix} \otimes \mathbf{G} \quad (4)$$

249 The off-diagonal elements represent variance for each trait and covariances between traits are the
250 off-diagonal elements.

251 Further, the residual term for each n-th trait is assumed to follow multivariate normal distribution:

252 $[\boldsymbol{\varepsilon}_1 \dots \boldsymbol{\varepsilon}_n] \sim N[0, (\mathbf{I} \otimes \mathbf{R})]$, where \mathbf{I} is the same as above and \mathbf{R} is a heterogeneous diagonal matrix
253 of the residual variances for each n-th trait:

254

255

$$\mathbf{R} = \begin{bmatrix} \sigma_{\varepsilon_1}^2 & 0 & \cdots & 0 \\ 0 & \sigma_{\varepsilon_2}^2 & \cdots & 0 \\ \vdots & \vdots & \ddots & \vdots \\ 0 & 0 & \cdots & \sigma_{\varepsilon_n}^2 \end{bmatrix} \otimes \mathbf{I} \quad (5)$$

256

257 The diagonal elements represent the residual variance for each n-th trait and off-diagonal elements
258 of the \mathbf{R} matrix equal zero. In our preliminary analysis unstructured \mathbf{R} matrix where off-diagonal
259 element of \mathbf{R} represent covariance of the residual effects of the traits was considered; however, we
260 observed inconsistent model convergence for all iterations. The same results were observed when
261 factor analytic model was considered for the \mathbf{R} structure which might be due to size of the dataset
262 used in our study relative to the number of model parameters to estimate.

263 Genomic heritability estimate (de los Campos et al. 2015; Feldmann et al. 2021) for n-th trait using
264 individual level data was derived from the variance components obtained from the model using
265 the complete dataset.

266

$$h_{g_n}^2 = \frac{\sigma_{g_n}^2}{\sigma_{g_n}^2 + \sigma_{\varepsilon_n}^2} \quad (6)$$

267 where $\sigma_{g_n}^2$ and $\sigma_{\varepsilon_n}^2$ are the genetic, residual variance estimates for n-th trait.

268

269

270

271 2.4 Cross-Validation Scheme

272 To evaluate the performance of sparse testing strategy in the context of MT-GS, different cross-
273 validations mimicking potential applications of MT-GS in a breeding program were explored.
274 Leveraging on the results from sparse testing in multi-environment yield trials using GS (Jarquin
275 et al. 2020; Atanda et al. 2021b), we varied the number of genotypes that serve as connectivity
276 across traits to assess predictive ability in the different scenarios. Depending on the size of the data
277 set and the number of phenotypes, different overlapping sizes were evaluated (**Suppl. Table 1**).
278 Five different overlapping sizes (50, 60, 70, 80, 90%) were considered for DS1 (n=282), which
279 had the highest total number of genotypes, followed by four overlapping sizes (40, 50, 60, 70%)
280 in DS2 (n=192). For example, when 50% of the total genotypes in DS1 serve as connectivity across
281 the traits, the remaining 141 genotypes were partitioned into 10 distinct sets, each trait with a
282 unique set. Thus, each trait has 155 genotypes as training set to predict the genetic merit of 127
283 genotypes (**Suppl. Figure 1B**). This process was repeated 50 times. As the size of the overlapping
284 genotypes increased (60, 70, 80, and 90% of total genotypes), the training set size increased to
285 180, 205, 230, 255, and the prediction set size reduced to 102, 77, 27 respectively. The splitting of
286 the genotypes across traits was also repeated 50 times for each overlapping size scenario, each
287 iteration has different genotypes that serve as connectivity across traits, non-overlapping training
288 set for each trait and the prediction set (**Suppl. Table 1**). In each iteration, the Pearson correlation
289 of the predicted GEBV and the BLUE estimates of the genotypes for each trait obtained using
290 complete dataset was calculated and the mean was recorded as the predictive ability of the
291 prediction set for each trait. The same process was repeated for DS2, however, the predictive
292 ability in each iteration is the Pearson correlation of the predicted GEBV obtained using complete
293 dataset and the mean phenotypic value of each accession for each trait and the mean was
294 recorded.

295

296 To determine the efficiency of MT (sparse and partially balanced phenotyping) and univariate
297 (UNI) GS model, we compared the predictive ability of the prediction sets using the different
298 training set size defined in each dataset. Again, this process was repeated 50 times, each iteration
299 having different genotypes included in the training and prediction set for all traits in the UNI-GS
300 model and across traits for the partially balanced phenotyping MT-GS. For sparse phenotyping
301 each iteration has different genotypes that serve as connectivity across traits, a non-overlapping
302 training set for each trait, and the prediction set (**Suppl. Figure 1**). For DS1, predictive ability for
303 each iteration was measured as the Pearson correlation of the predicted GEBV and the BLUE
304 estimates of the genotypes for each trait obtained using the full dataset. Average was reported. In
305 the DS2, BLUE was replaced with the mean phenotypic value of each accession for each trait.

306

307 Based on the preliminary analysis results, only the sparse testing using MT-GS was considered to
308 evaluate the efficiency of using heritability, genetic correlation between traits or combination of
309 the factors for trait assignment in the prediction set and/or training set respectively. The following
310 scenarios were assessed:

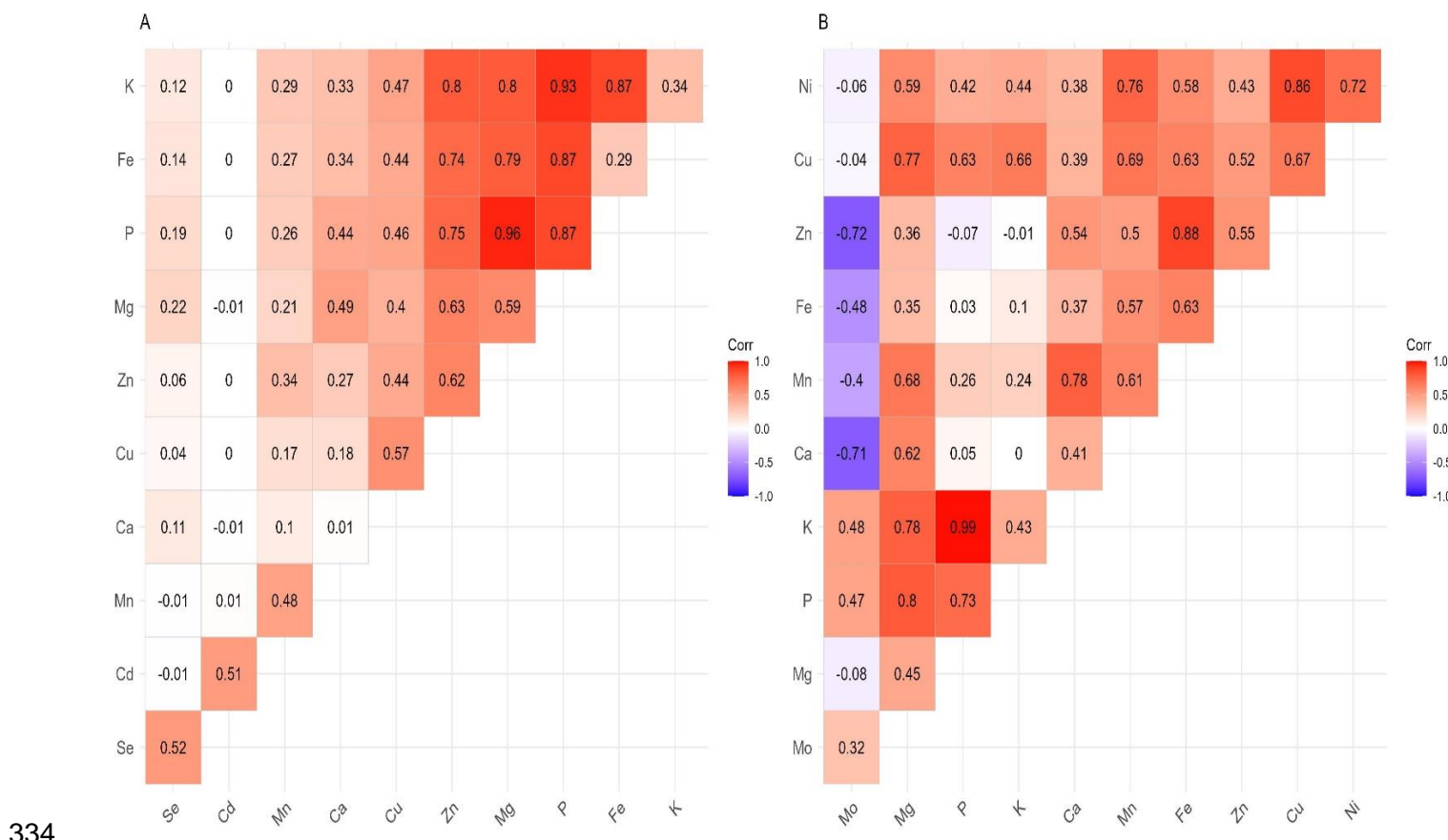
- 311 1) Exclusion of trait(s) with lowest heritability but moderate to high genetic correlation
312 with other traits from the prediction set however reserved in the model. We also evaluated
313 the scenario when it was removed from the model.
- 314 2) Exclusion of trait(s) with the highest occurrence of negative correlation with other traits
315 but moderate to high heritability from the prediction set but reserved in the model. We also
316 evaluated the scenario when it was removed from the model.
- 317 3) Exclusion of trait(s) with the lowest heritability but moderate to high genetic correlation
318 with other traits, as well as trait(s) with the highest occurrence of negative correlation with

319 other traits but moderate to high heritability, from the prediction set but reserved in the
320 model. We also evaluated the scenario in which they were left out of the model.

321 **3.0 Results**

322 **3.1 Traits genomic heritability (diagonal) and genetic correlation among traits (upper**
323 **diagonal)**

324 In DS1 heritability was moderately high for all traits except Ca with very low heritability value of
325 0.01 (**Fig. 1A**). However, in DS2 Ca had moderate heritability of 0.40 (**Fig. 1B**). Similarly, Fe had
326 heritability of 0.63 in DS2 compared to 0.29 in DS1, and in general the traits heritability in DS2
327 ranged from moderate to high. In the two datasets, P consistently had the highest heritability of
328 0.87 in DS1 and 0.73 in DS2. The genetic correlation between traits in DS1 ranged from -0.01 to
329 0.96 while it ranged from -0.01 to 0.99 in DS2. In DS1, Cd had zero or no genetic correlation with
330 most of the traits. Similarly, K had no genetic correlation with Ca in DS2, contrary to the 0.33
331 genetic correlation observed in DS1 (**Fig. 1A, B**). Generally, in DS1, K, Fe, P and Mg had
332 moderate to high genetic correlation with most of the traits while in DS2 Ni, Cu and Mg had high
333 genetic correlation with other traits except with Mo.



334

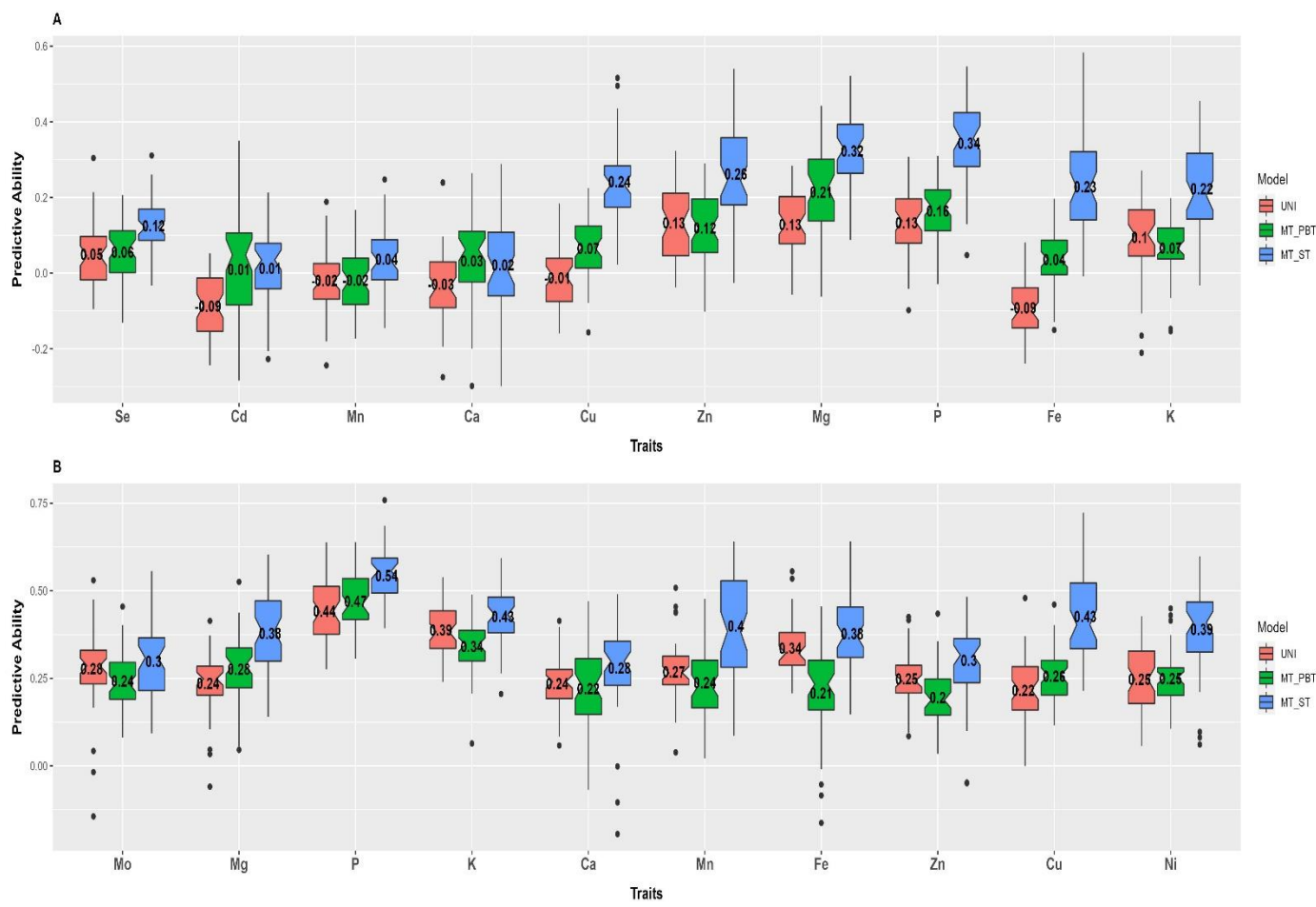
335 **Figure 1: Genomic heritability (diagonal) and genetic correlation between pairs of traits**
 336 **(upper diagonal) from MT-GS model using complete datasets. Fig. 1A, represent results**
 337 **using DS1 dataset and Fig. 1B indicate results using DS2 dataset.**

338

339 **3.2 Sparse testing MT-GS improves predictive ability across traits compared to partially**
 340 **balanced testing MT and univariate GS models.**

341 Regardless of cross-validation schemes or dataset, sparse testing MT-GS model outperformed PBT
 342 MT and UNI-GS models for all traits except for Ca in DS1 which might be attributed to near-zero
 343 genetic signal observed for this trait (**Fig. 2A: B**). For instance, in DS2 where the predictive ability
 344 is generally high compared to DS1, sparse testing using MT-GS outperformed PBT using MT-GS
 345 by 25, 36, 15, 26, 27, 67, 81, 50, 66, 56% respectively for Mo, Mg, P, K, Ca, Mn, Fe, Zn, Cu and

346 Ni while it improved predictive ability by 7, 58, 23, 17, 60, 12, 2, 95, 56% compared to UN-GS
347 model (**Fig. 2B**). Surprisingly, PBT using MT-GS model did not consistently outperform UNI-GS
348 model in DS2 compared to DS1 where PBT using MT-GS marginally results in improved
349 predictive ability for all traits.



350

351 **Figure 2: Predictive performance of UNI and MT-GS using partially balanced (PBT) and**

352 sparse testing (ST) phenotyping of the traits. The number within each box represents mean

353 predictive ability of 50 iterations of the process of line assignment as training and prediction

354 set. In each iteration different genotypes were assigned as training and prediction set for the

355 traits in the UNI-GS model and across traits for the partially balanced phenotyping MT-GS.

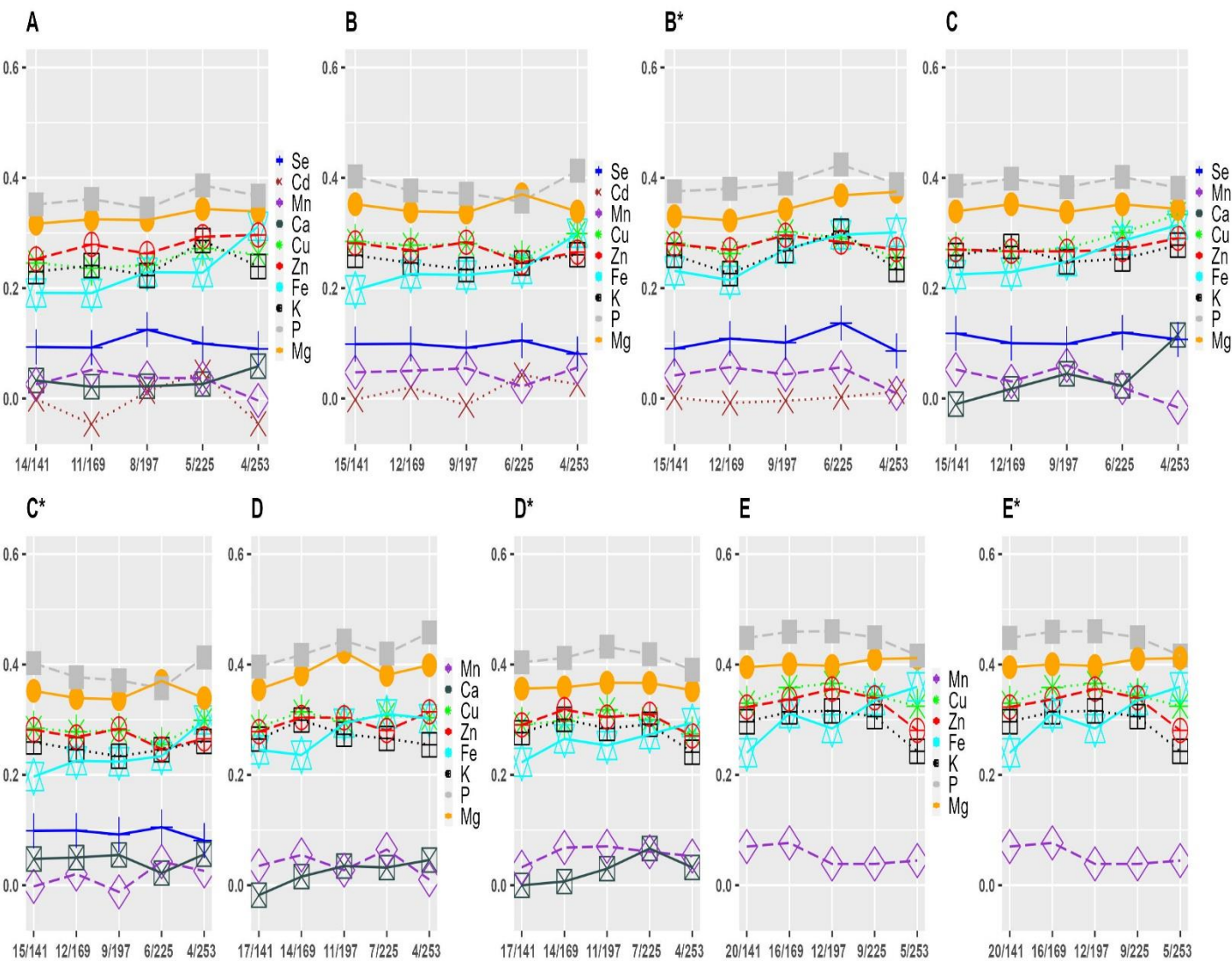
356 For sparse phenotyping each iteration has different genotypes that serve as connectivity

357 across traits, a non-overlapping training set for each trait, and the prediction set

358 **3.2 Traits combination as a function of heritability, genetic correlation between traits and**
359 **their combination**

360 When either heritability or genetic correlation was considered a decision tool for a combination of
361 traits in the prediction and/or calibration set, the predictive ability improved for all traits compared
362 to having all the traits in the prediction and the training set. However, the magnitude of the gain in
363 predictive ability varies by trait (**Fig. 3, 4**). In DS1, for example, when Ca with the lowest
364 heritability (0.01) but moderate to high genetic correlation with other traits was dropped from the
365 prediction set but kept in the model, the gain in the predictive ability for the remaining 9 traits in
366 the prediction set across the overlapping scenarios ranged from 2.79 to 85.07% (**Fig. 3B**), while it
367 ranged from 3.28 to 63.37% when excluded from the model (**Fig. 3B***). When Cd with high
368 heritability (0.51) but zero genetic correlation with most traits was removed from the prediction
369 set, but retained in the calibration model, the improvement in predictive ability ranged from 6.75
370 to 104.41% (**Fig. 3C**) and ranged from 1.38 to 45.42% when removed from the training model
371 (**Fig. 3C***). Similar results were obtained in DS2, when Mo with heritability of 0.43 and negative
372 correlation with the majority of the traits was removed from the prediction set but reserved in the
373 calibration model. The predictive ability of traits in the prediction set ranged from 2.41 to 77.92%
374 (**Fig. 4B**) and ranged from 0.62 to 19.62% when removed from the model (**Fig. 4B***). Because Mo
375 has a negative genetic correlation with the majority of the traits, in addition to having the lowest
376 heritability of all the traits in DS2, we substitute Mo with Ca, which has a heritability of 0.41 and
377 a moderate to high genetic correlation with other traits, to disentangle the confounding effect of
378 heritability and genetic correlation. The gain in predictive ability ranged from 3.19 to 90.34%
379 when the calibration model was reserved (**Fig. 4C**) and from 1.34 to 14.65% when the calibration
380 model was removed (**Fig. 4C***).

381 Unsurprisingly, when Mo and P, which have moderate and high heritabilities of 0.32 and 0.73 but
382 are negatively correlated with other traits, respectively, were excluded from the prediction set, the
383 predictive ability improved for all traits except Ca and Fe (**Fig. 4D**). When the traits were removed
384 from the calibration model, the predictive ability decreased for majority of the traits (**Fig. 4D***).
385 On the contrary, removing Mo and K from the prediction set with moderate heritability of 0.32
386 and 0.43 resulted in an improved predictive ability (**Fig. 4E, E***). In contrast to P, K has zero,
387 weak negative, and strong positive correlations with other traits. Figures 3D and 3D* corroborate
388 the findings in Figures 4D and 4D*, in which Se and Cd with moderate heritability of 0.51 and
389 0.52, respectively, but low genetic correlation with other traits, were excluded from the prediction
390 set but retained or removed from the calibration model. The additional improvement in predictive
391 ability observed when Se, Cd, and Ca were excluded from the prediction set (**Fig. 3E, E***)
392 demonstrates the efficacy of heritability and genetic correlation between traits as decision metric,
393 corroborating the results obtained in Figure 4E and 4E*.

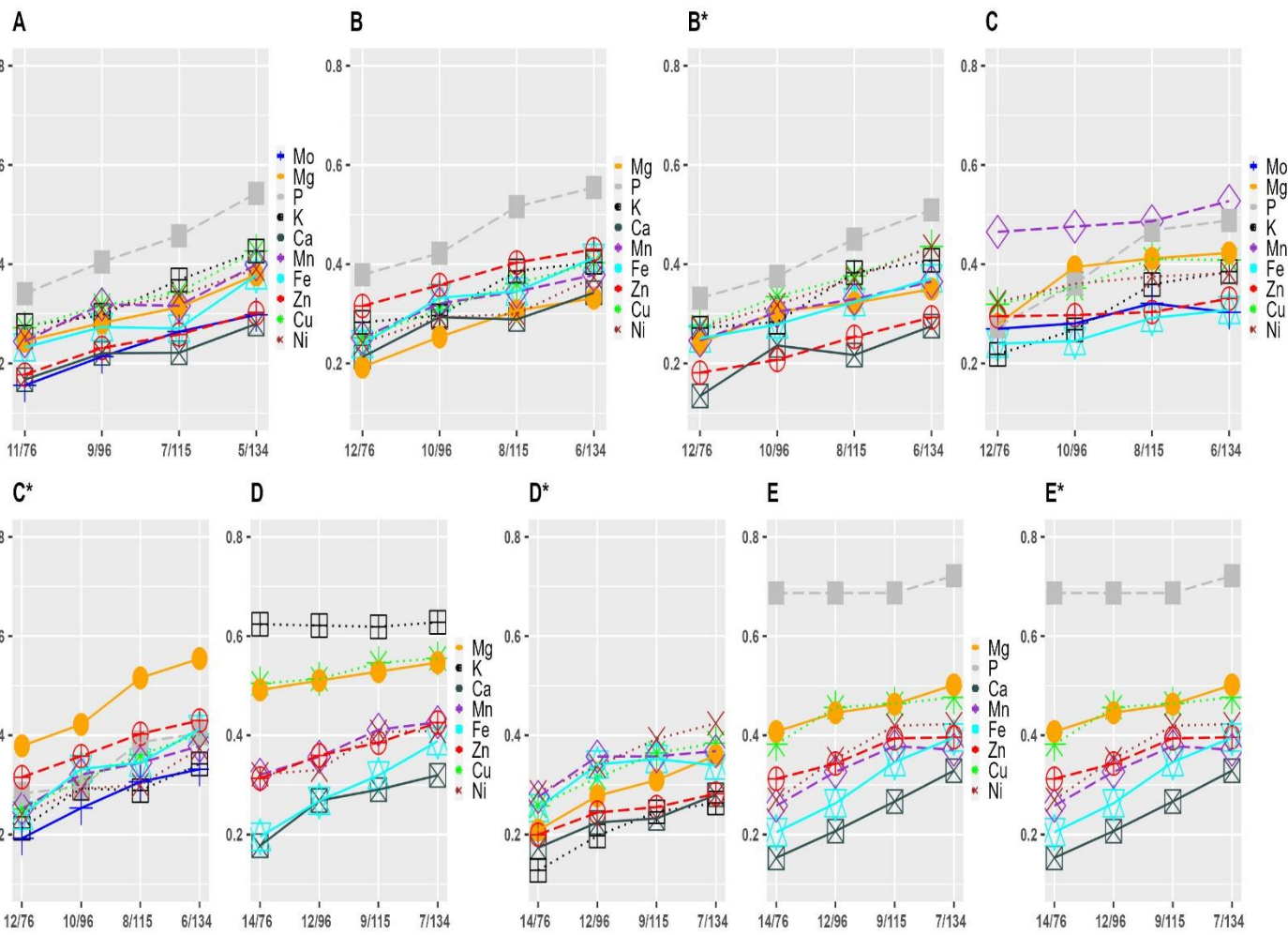


394

395 **Figure 3: Predictive ability of untested lines in DS1 for each trait for different overlapping**
 396 **and non-overlapping size. The different colors denote traits in the prediction set, which might**
 397 **also be present in the calibration model. The suffix (*) indicate exclusion of trait (s) from the**
 398 **calibration model based on its heritability, degree of genetic correlation with other traits or**
 399 **combination of the two factors.**

400

401



402

403 **Figure 4: Predictive ability of untested lines in DS2 for each trait for different overlapping**
 404 **and non-overlapping size. The different colors denote traits in the prediction set, which might**
 405 **also be present in the calibration model. The suffix (*) indicate exclusion of trait (s) from the**
 406 **calibration model based on its heritability, degree of genetic correlation with other traits or**
 407 **combination of the two factors.**

408

409

410

411

412 4.0 Discussion

413 Breeders make advancement decisions based on multiple traits with varying genetic correlations,
414 ranging from negative to positive, and in exceptional cases, no genetic correlation at all. Thus, the
415 use of the MT-GS model is gaining popularity as a choice GS model to estimate the genetic merit
416 of new genotypes. When comparing models, our results corroborate previous studies (Calus and
417 Veerkamp 2011; Jia and Jannink 2012; Montesinos-López et al. 2018; Lado et al. 2018; Bhatta et
418 al. 2020; Gaire et al. 2022) that MT-GS outperforms UNI-GS by harnessing genetic correlation
419 between traits to improve predictive ability across traits. The proposed MT-GS aided sparse
420 phenotyping depart from the previous reports of weak genetic correlation between traits as a
421 limitation to the advantage of MT-GS over UNI, which was evident in the partially balanced
422 phenotyping aided MT-GS. The performance of MT-GS enabled sparse phenotyping was
423 consistently superior to UNI-GS, with least 20% improvement on predictive ability on average
424 across traits, suggesting the importance of borrowing information across traits and related
425 genotypes. Similar results have been reported in sparse testing aided GS in multi-environment
426 trials (Atanda et al. 2021a; 2021b; 2022). This demonstrates the improvement in predictive
427 performance in sparse testing using MT-GS is primarily due to efficient estimation of correlated
428 effects across genetically related traits, as phenotypic records are available for all traits, albeit in a
429 different set of genotypes. In addition, allowing for significant genotype overlap improves
430 predictive ability because genetic connectivity across traits improves estimates of trait-to-trait
431 correlation effects. The observed inflection points in this study, however, suggests that more
432 research is required to determine the optimal number of overlapping genotypes, which might be
433 influenced by the degree of genetic relationship between lines, the number of lines per cross, the
434 genetic correlation between traits, yield testing stage and expected prediction accuracy.

435

436 Overall, predictive ability improves with heritability in all models except Se, Cd, and Mn in DS1,
437 though DS1 generally has low predictive ability compared to DS2, presumably due to low genetic
438 variation for nutritional traits in DS1 which are elite breeding lines compared to DS2 which are
439 accessions and the growing condition of the accessions in the greenhouse compared to DS1 planted
440 out in the field. Thavarajah et al. (2022) reported heritability estimates of nearly zero for Ca, K, P,
441 Mg, Mn, Fe, Zn, Cu and Se in 44 pea lines evaluated in two locations in 2019 and one location in
442 2020 with two replications in each location. On the contrary, Ma et al. (2017) observed moderately
443 high genetic diversity for mineral elements in 158 recombinant inbred lines evaluated in two
444 locations with two replications. Given the number of replications and locations used in these
445 studies further suggests that the degree of genetic variation (by inference heritability) for
446 nutritional traits in DS1 may be responsible for the observed low predictive ability.

447

448 Multi-trait combinations were created in training and prediction sets based on genetic correlations
449 between traits, heritability, and the combination of the limiting factors to optimize the trade-off
450 between the limiting factors and the accuracy of predicting the genetic value of the phenotypes. In
451 general, the improvement in predictive ability when traits with low heritability but moderate to
452 high genetic correlation with other traits or traits with high occurrence of negative correlation with
453 other traits but moderate to high heritability were excluded from the prediction set suggests that
454 traits with low heritability or genetic correlation with other traits cannot be adequately predicted
455 (Jia and Jannink 2012; Gaire et al. 2022). However, reserving the traits in the training set as
456 secondary traits improves estimation of model parameters resulting in an improvement in
457 predictive ability compared to exclusion from the model. The observed difference in predictive
458 ability for each limiting factor suggests both factors independently affects predictive ability.
459 Consequently, both factors are equally important in determining traits combination in MT-GS. In
460 practice, this information can be sourced from relevant literature on the phenotypes or historical

461 data in the breeding program. To our knowledge this is the first time these two factors are designed
462 to designate traits in the training and prediction set to improve predictive performance in MT-GS.
463 The gain in predictive performance achieved by using this strategy requires further investigation
464 because it has only been tested in pea datasets with limited environments (year by location
465 combinations) and replication which is a major limitation in this study, and does not represent
466 extensive data generated in breeding programs. The availability of multi-environment dataset can
467 improve estimate of genotypic values for quantitative traits. Since significant progress has been
468 made in multi-trait multi-environment genomic prediction (Montesinos-López et al. 2016, 2018,
469 2019; Gill et al. 2021; Sandhu et al. 2022), our findings suggest future research should focus on
470 developing an optimal strategy for genomic prediction enabled sparse testing of multiple traits in
471 multi-environment trials. This will likely further lower the cost of phenotyping and the time-
472 consuming data collection process. In addition, we encourage use of different crops with varying
473 genetic backgrounds that fairly cover the diversity of data generated in breeding programs to gather
474 more evidence on the efficiency of this strategy in improving prediction performance in MT-GS.

475

476 Conclusion

477 In this study we propose use of sparse testing in MT-GS which ultimately can be extended to multi-
478 environment multi-trait GS to improve prediction performance and further reduce the cost of
479 phenotyping and time-consuming data collection process. Although our results agree with previous
480 study that weak correlation is a limiting factor of MT-GS superiority over UNI-GS using partially
481 balanced phenotyping. However, our results were inconsistent with sparse phenotyping,
482 suggesting that MT-GS performance can be improved further if phenotyping strategy is
483 redesigned. Our results show that traits combination in training and prediction sets impact
484 prediction performance. Therefore, when designing MT-GS strategy, consideration should be

485 given to traits combination in the training and prediction sets. In addition, our results suggest the
486 use of heritability and genetic correlation between traits as metrics to achieve this objective.

487

488

489

490

491 **Data Availability Statement**

492 The SNP dataset used in this study is available via:
493 <https://www.ncbi.nlm.nih.gov/sra/PRJNA730349>. And the phenotypic data will be made available
494 by reaching out to the corresponding author.

495

496 **Author Contributions**

497 SA and NB conceptualized the study. SA performed the analyses, and wrote the manuscript. HW,
498 AR, MM, JK, and MAB coordinated the field experiments for the NDSU breeding lines.
499 LP, JS, JJ and RAS coordinated the genotyping experiments for the NDSU breeding lines. JR, YL,
500 JS, and LP coordinated the mineral profiling of the NDSU breeding lines. MAG, CJC, and RJM
501 designed and executed the greenhouse experiment, genotyping, and mineral profiling of the USDA
502 accessions. NB oversaw the statistical analyses and contributed to the writing of the manuscript.
503 All authors edited, reviewed, and approved the manuscript.

504

505 **Conflict of Interest**

506 The authors declare that the study was conducted in the absence of any commercial or financial
507 relationships that could be construed as a potential conflict of interest.

508

509 **Acknowledgments**

510 This research was supported through funding from USDA Plant Genetic Resource Evaluation,
511 USA Dry Pea and Lentil Council Research Committee, USDA ARS Pulse Crop Health Initiative

512 and USDA ARS Project: 5348-21000-017-00D (CC), and 5348-21000-024-00D (RJM). Also,
513 grants from USDA-NIFA (Hatch Project ND01513 for NB) and the North Dakota Department of
514 Agriculture through the Specialty Crop Block Grant Program (19-429).

515

516

517 **References**

518 Annicchiarico, Paolo, Nelson Nazzicari, Luciano Pecetti, Massimo Romani, and Luigi Russi.
519 2019. Pea Genomic Selection for Italian Environments. *BMC Genomics* 20 (1): 603.

520 Atanda, Sikiru Adeniyi, Veli Govindan, Ravi Singh, Kelly R. Robbins, Jose Crossa, and Alison
521 R. Bentley. 2022. Sparse Testing Using Genomic Prediction Improves Selection for Breeding
522 Targets in Elite Spring Wheat. *TAG. Theoretical and Applied Genetics*.
523 <https://doi.org/10.1007/s00122-022-04085-0>.

524 Atanda, Sikiru Adeniyi, Michael Olsen, Juan Burgueño, Jose Crossa, Daniel Dzidzienyo, Yoseph
525 Beyene, Manje Gowda, et al. 2021. Maximizing Efficiency of Genomic Selection in
526 CIMMYT's Tropical Maize Breeding Program. *TAG. Theoretical and Applied Genetics*.
527 *Theoretische Und Angewandte Genetik* 134 (1): 279–94.

528 Atanda, Sikiru Adeniyi, Michael Olsen, Jose Crossa, Juan Burgueño, Renaud Rincent, Daniel
529 Dzidzienyo, Yoseph Beyene, et al. 2021. Scalable Sparse Testing Genomic Selection Strategy
530 for Early Yield Testing Stage. *Frontiers in Plant Science* 12 (June): 658978.

531 Bari, Md Abdullah Al, Ping Zheng, Indalecio Viera, Hannah Worral, Stephen Szwiec, Yu Ma,
532 Dorrie Main, Clarice J. Coyne, Rebecca J. McGee, and Nonoy Bandillo. 2021. Harnessing
533 Genetic Diversity in the USDA Pea Germplasm Collection Through Genomic Prediction.
534 *Frontiers in Genetics* 12 (December): 707754.

535 Bassi, Filippo M., Alison R. Bentley, Gilles Charmet, Rodomiro Ortiz, and Jose Crossa. 2016.
536 Breeding Schemes for the Implementation of Genomic Selection in Wheat (*Triticum* Spp.).

537 *Plant Science: An International Journal of Experimental Plant Biology* 242 (January): 23–
538 36.

539 Bhatta, Madhav, Lucia Gutierrez, Lorena Cammarota, Fernanda Cardozo, Silvia Germán, Blanca
540 Gómez-Guerrero, María Fernanda Pardo, Valeria Lanaro, Mercedes Sayas, and Ariel J.
541 Castro. 2020. Multi-Trait Genomic Prediction Model Increased the Predictive Ability for
542 Agronomic and Malting Quality Traits in Barley (L.). *G3* 10 (3): 1113–24.

543 Browning, Brian L., Ying Zhou, and Sharon R. Browning. 2018. A One-Penny Imputed Genome
544 from Next-Generation Reference Panels. *American Journal of Human Genetics* 103 (3): 338–
545 48.

546 Burgueño, Juan, Gustavo de los Campos, Kent Weigel, and José Crossa. 2012. Genomic Prediction
547 of Breeding Values When Modeling Genotype × Environment Interaction Using Pedigree
548 and Dense Molecular Markers. *Crop Science*. <https://doi.org/10.2135/cropsci2011.06.0299>.

549 Calus, Mario P. L., and Roel F. Veerkamp. 2011. Accuracy of Multi-Trait Genomic Selection
550 Using Different Methods. *Genetics, Selection, Evolution: GSE* 43 (July): 26.

551 Crossa, J., Perez-Rodriguez, P., Cuevas, J., Montesinos-Lopez, O., Jarquin, D., de Los Campos,
552 G., Burgueno, J. et al. (2017) Genomic selection in plant breeding: methods, models, and
553 perspectives. *Trends Plant Sci.* 22, 961–975.

554 Crosta, Margherita, Nelson Nazzicari, Barbara Ferrari, Luciano Pecetti, Luigi Russi, Massimo
555 Romani, Giovanni Cabassi, Daniele Cavalli, Adriano Marocco, and Paolo Annicchiarico.
556 2021. Pea Grain Protein Content Across Italian Environments: Genetic Relationship With
557 Grain Yield, and Opportunities for Genome-Enabled Selection for Protein Yield. *Frontiers
558 in Plant Science* 12: 718713.

559 de los Campos, G. and A. Grüneberg. 2016. MTM Package.
560 <http://quantgen.github.io/MTM/vignette.html>.

561 de los Campos, G., Daniel Sorensen, and Daniel Gianola. 2015. Genomic Heritability: What Is It?

562 *PLOS Genetics*. <https://doi.org/10.1371/journal.pgen.1005048>.

563 Feldmann, Mitchell J., Hans-Peter Piepho, and Steven J. Knapp. n.d. 2021. Genomic Heritability:

564 A Ragged Diagonal Between Bias and Variance. <https://doi.org/10.1101/2021.09.19.460999>.

565 Gaire, Rupesh, Marcio Pais de Arruda, Mohsen Mohammadi, Gina Brown-Guedira, Frederic L.

566 Kolb, and Jessica Rutkoski. 2022. Multi-Trait Genomic Selection Can Increase Selection

567 Accuracy for Deoxynivalenol Accumulation Resulting from Fusarium Head Blight in Wheat.

568 *The Plant Genome*, January, e20188.

569 Gill, Harsimardeep S., Jyotirmoy Halder, Jinfeng Zhang, Navreet K. Brar, Teerath S. Rai, Cody

570 Hall, Amy Bernardo, et al. 2021. “Multi-Trait Multi-Environment Genomic Prediction of

571 Agronomic Traits in Advanced Breeding Lines of Winter Wheat.” *Frontiers in Plant Science*

572 12 (August): 709545.

573 Guo, Gang, Fuping Zhao, Yachun Wang, Yuan Zhang, Lixin Du, and Guosheng Su. 2014.

574 Comparison of Single-Trait and Multiple-Trait Genomic Prediction Models. *BMC Genetics*

575 15 (March): 30.

576 Jarquin, Diego, Reka Howard, Jose Crossa, Yoseph Beyene, Manje Gowda, Johannes W. R.

577 Martini, Giovanny Covarrubias Pazaran, et al. 2020. Genomic Prediction Enhanced Sparse

578 Testing for Multi-Environment Trials. *G3* 10 (8): 2725–39.

579 Jia, Yi, and Jean-Luc Jannink. 2012. Multiple-Trait Genomic Selection Methods Increase Genetic

580 Value Prediction Accuracy. *Genetics* 192 (4): 1513–22.

581 Lado, Bettina, Daniel Vázquez, Martin Quincke, Paula Silva, Ignacio Aguilar, and Lucia

582 Gutiérrez. 2018. Resource Allocation Optimization with Multi-Trait Genomic Prediction for

583 Bread Wheat (*Triticum Aestivum* L.) Baking Quality. TAG. Theoretical and Applied

584 Genetics. *Theoretische Und Angewandte Genetik* 131 (12): 2719–31.

585 Lan, Yang, Fengchao Zha, Allen Peckrul, Bryan Hanson, Burton Johnson, Jiajia Rao, and Bingcan

586 Chen. 2019. Genotype X Environmental Effects on Yielding Ability and Seed Chemical

587 Composition of Industrial Hemp (*Cannabis Sativa L.*) Varieties Grown in North Dakota,
588 USA. *Journal of the American Oil Chemists' Society*. <https://doi.org/10.1002/aocs.12291>.

589

590 Ma, Yu, Clarice J. Coyne, Michael A. Grusak, Michael Mazourek, Peng Cheng, Dorrie Main, and
591 Rebecca J. McGee. 2017. Genome-Wide SNP Identification, Linkage Map Construction and
592 QTL Mapping for Seed Mineral Concentrations and Contents in Pea (*Pisum Sativum L.*).
593 *BMC Plant Biology* 17 (1): 43.

594 Manolio, Teri A., Francis S. Collins, Nancy J. Cox, David B. Goldstein, Lucia A. Hindorff, David
595 J. Hunter, Mark I. McCarthy, et al. 2009. Finding the Missing Heritability of Complex
596 Diseases. *Nature*. <https://doi.org/10.1038/nature08494>.

597 Montesinos-López, Osval A., Abelardo Montesinos-López, José Crossa, Jaime Cuevas, José C.
598 Montesinos-López, Zitlalli Salas Gutiérrez, Morten Lillemo, Juliana Philomin, and Ravi
599 Singh. 2019. A Bayesian Genomic Multi-Output Regressor Stacking Model for Predicting
600 Multi-Trait Multi-Environment Plant Breeding Data. *G3* 9 (10): 3381–93.

601 Montesinos-López, Osval A., Abelardo Montesinos-López, José Crossa, Daniel Gianola, Carlos
602 M. Hernández-Suárez, and Javier Martín-Vallejo. 2018. Multi-Trait, Multi-Environment
603 Deep Learning Modeling for Genomic-Enabled Prediction of Plant Traits. *G3* 8 (12): 3829–
604 40.

605 Montesinos-López, Osval A., Abelardo Montesinos-López, José Crossa, Fernando H. Toledo,
606 Oscar Pérez-Hernández, Kent M. Eskridge, and Jessica Rutkoski. 2016. A Genomic Bayesian
607 Multi-Trait and Multi-Environment Model. *G3* 6 (9): 2725–44.

608 Mudryj, Adriana N., Nancy Yu, and Harold M. Aukema. 2014. Nutritional and Health Benefits of
609 Pulses. *Applied Physiology, Nutrition, and Metabolism = Physiologie Appliquée, Nutrition et*
610 *Metabolisme* 39 (11): 1197–1204.

611 Neyhart, Jeffrey L., Aaron J. Lorenz, and Kevin P. Smith. 2019. Multi-Trait Improvement by

612 Predicting Genetic Correlations in Breeding Crosses. *G3* 9 (10): 3153–65.

613 Okeke, Uche Godfrey, Deniz Akdemir, Ismail Rabbi, Peter Kulakow, and Jean-Luc Jannink. 2017.

614 Accuracies of Univariate and Multivariate Genomic Prediction Models in African Cassava.

615 *Genetics, Selection, Evolution: GSE* 49 (1): 88.

616 Pérez, Paulino, and Gustavo de los Campos. 2014. Genome-Wide Regression and Prediction with

617 the BGLR Statistical Package. *Genetics* 198 (2): 483–95.

618 Poland, Jesse, Jeffrey Endelman, Julie Dawson, Jessica Rutkoski, Shuangye Wu, Yann Manes,

619 Susanne Dreisigacker, et al. 2012. Genomic Selection in Wheat Breeding Using Genotyping-

620 by-Sequencing. *The Plant Genome*. <https://doi.org/10.3835/plantgenome2012.06.0006>.

621 Rodríguez-Álvarez MX, Boer MP, Eilers PHC, van Eeuwijk FA. 2016. SpATS: spatial analysis

622 of field trials with splines. R package version 1.0–4. <https://cran.r-project.org/package=SpATS>

623

624 Sandhu, Karansher S., Shruti Sunil Patil, Meriem Aoun, and Arron H. Carter. 2022. “Multi-Trait

625 Multi-Environment Genomic Prediction for End-Use Quality Traits in Winter Wheat.”

626 *Frontiers in Genetics*. <https://doi.org/10.3389/fgene.2022.831020>.

627 Santantonio, Nicholas, Sikiru Adeniyi Atanda, Yoseph Beyene, Rajeev K. Varshney, Michael

628 Olsen, Elizabeth Jones, Manish Roorkiwal, et al. 2020. Strategies for Effective Use of

629 Genomic Information in Crop Breeding Programs Serving Africa and South Asia. *Frontiers*

630 in *Plant Science* 11 (March): 353.

631 Schopp, Pascal, Dominik Müller, Yvonne C. J. Wientjes, and Albrecht E. Melchinger. 2017.

632 Genomic Prediction Within and Across Biparental Families: Means and Variances of

633 Prediction Accuracy and Usefulness of Deterministic Equations. *G3* 7 (11): 3571–86.

634 Thavarajah, Dil, Tristan J. Lawrence, Sarah E. Powers, Joshua Kay, Pushparajah Thavarajah,

635 Emerson Shipe, Rebecca McGee, Shiv Kumar, and Rick Boyles. 2022. Organic Dry Pea

636 (*Pisum Sativum L.*) Biofortification for Better Human Health. *PloS One* 17 (1): e0261109.

637 Velazco, Julio G., María Xosé Rodríguez-Álvarez, Martin P. Boer, David R. Jordan, Paul H. C.
638 Eilers, Marcos Malosetti, and Fred A. van Eeuwijk. 2017. Modelling Spatial Trends in
639 Sorghum Breeding Field Trials Using a Two-Dimensional P-Spline Mixed Model. TAG.
640 Theoretical and Applied Genetics. Theoretische Und Angewandte Genetik 130 (7): 1375–92.
641 Wadhawan, Nikita, Chavan Sagar Madhukar, and Gaurav Wadhawan. 2021. Nutraceutical and
642 Health Benefits of Pulses. *Handbook of Cereals, Pulses, Roots, and Tubers.*
643 <https://doi.org/10.1201/9781003155508-30>.

644 Yang, Jian, Andrew Bakshi, Zhihong Zhu, Gibran Hemani, Anna A. E. Vinkhuyzen, Sang Hong
645 Lee, Matthew R. Robinson, et al. 2015. Genetic Variance Estimation with Imputed Variants
646 Finds Negligible Missing Heritability for Human Height and Body Mass Index. *Nature*
647 *Genetics* 47 (10): 1114–20.

648 Zhang, Haohao, Lilin Yin, Meiyue Wang, Xiaohui Yuan, and Xiaolei Liu. 2019. Factors Affecting
649 the Accuracy of Genomic Selection for Agricultural Economic Traits in Maize, Cattle, and
650 Pig Populations. *Frontiers in Genetics* 10 (March): 189.

651 Zhao, Changheng, Jun Teng, Xinhao Zhang, Dan Wang, Xinyi Zhang, Shiyin Li, Xin Jiang,
652 Haijing Li, Chao Ning, and Qin Zhang. 2021. Towards a Cost-Effective Implementation of
653 Genomic Prediction Based on Low Coverage Whole Genome Sequencing in Dezhou Donkey.
654 *Frontiers in Genetics* 12 (November): 728764.

655

656

657

658

659

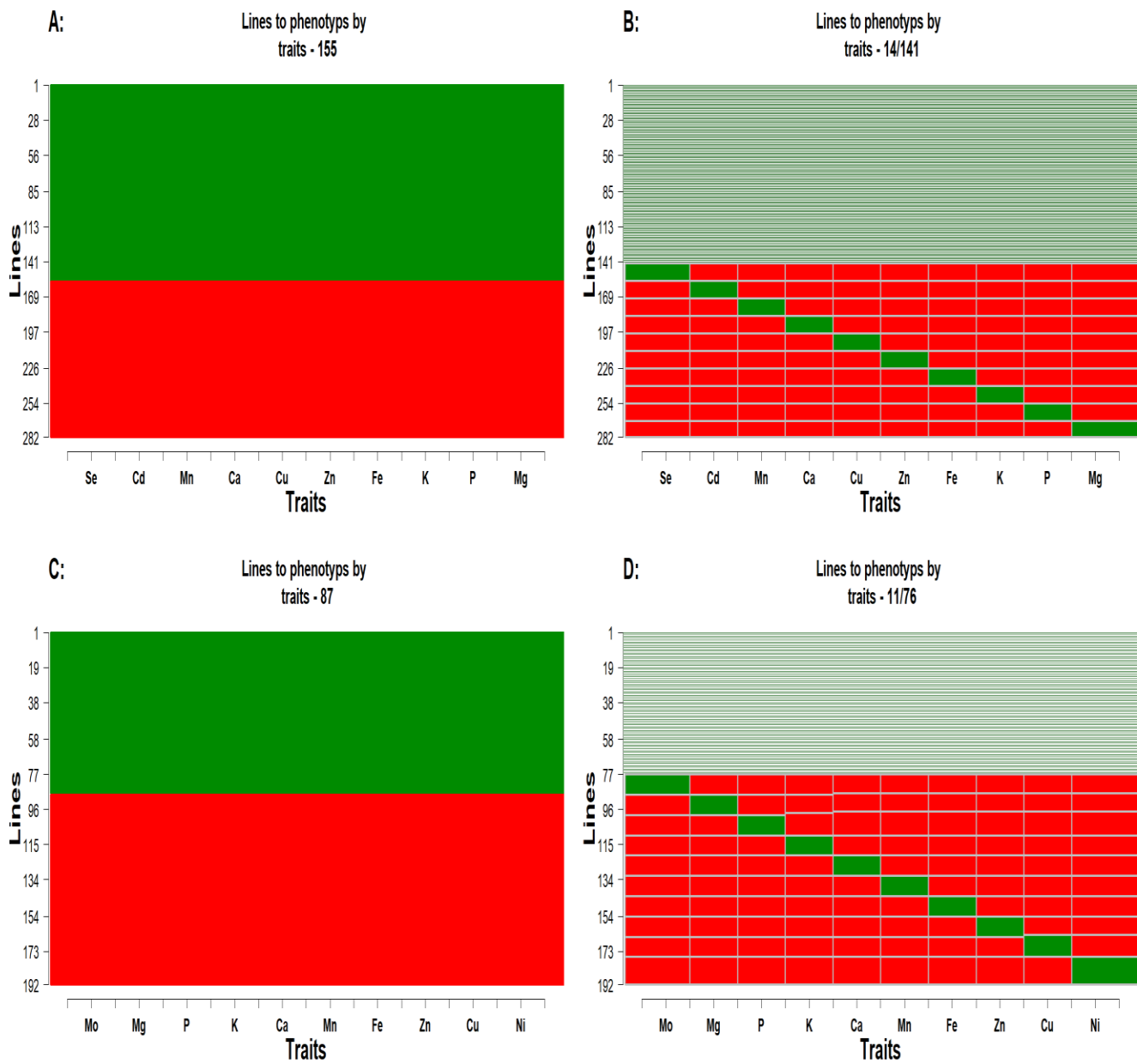
660

661

662 **Supplementary Table 1: Proportion of genotypes overlapping and non-overlapping across**
 663 **traits for DS1 and DS2 datasets**

	Total # of genotypes	# of Traits	Percent overlap across traits	Overlapping across traits	Non-Overlapping	Total Training set size	Testing set size
DS1	282	10	50	141	14:15	155:156	126:127
	282	10	60	169	11:12	179:180	102:103
	282	10	70	197	8:9	205:206	76:77
	282	10	80	225	5:6	230:231	52:51
	282	10	90	253	2:3	255:256	26:27
	282	9	50	141	15:16	156:157	125:126
	282	9	60	169	12:13	181:182	101:102
	282	9	70	197	9:10	206:207	75:76
	282	9	80	225	6:7	231:30	50:51
	282	9	90	253	3:4	256:257	25:26
	282	8	50	141	17:18	156:157	123:124
	282	8	60	169	14:15	183:184	99:98
	282	8	70	197	10:11	207:208	74:75
	282	8	80	225	7:8	232:233	49:50
	282	8	90	253	3:4	256:257	25:26
	282	7	50	141	20:21	161:162	120:121
	282	7	60	169	16:17	185:186	95:96
	282	7	70	197	12:13	204:205	77:78
	282	7	80	225	8:9	233:234	48:49
	282	7	90	253	4:5	257:258	24:25
DS2	192	10	40	76	11:12	87:88	104:105
	192	10	50	96	9:10	105:106	86:87
	192	10	60	115	7:8	122:123	69:70
	192	10	70	134	5:8	139:140	52:53
	192	9	40	76	12:13	88:89	103:104
	192	9	50	96	10:11	106:107	85:86
	192	9	60	115	8:9	123:124	68:69
	192	9	70	134	6:7	140:141	51:52
	192	8	40	76	14:15	90:91	101:102
	192	8	50	96	12	108:109	83:84
	192	8	60	115	9:10	124:125	67:68
	192	8	70	134	7:8	141:142	50:51

664
 665
 666 The symbol (:) between numbers implies when splitting the lines across the traits some traits might
 667 have the first value and others have the second value. Splitting of lines across the traits was
 668 repeated 50 times. DS1 includes 282 NDSU pea lines while DS2 includes 192 USDA accessions.
 669



670
671 **Supplementary Figure 1: Allocation of lines to 10 traits in DS1 (A and B) and DS2 (C and D)**
672 respectively. In A and C, the green section corresponds to 155 and 87 lines in DS1 and DS2
673 with phenotypic data for all traits using partially balanced phenotyping. While the red
674 implies un-phenotyped lines across traits in which the genetic value will be predicted. The
675 B and D are sparse phenotyping strategy, each column represents a trait and the green
676 sections correspond to 14 and 11 lines in DS1 and DS2 unique to each trait while the light

677 **green section denotes 141 and 76 lines (Approx. 50% of 282 lines in DS1 and 40% 192 lines**

678 **in DS2) common to all traits.**

679

680

681

682